CHAPTER IX

EFFECT OF SURFACE SITES (Ti^{3+} AND Ti^{4+}) OF TiO_2 SUPPORT ON THE FORMATION OF COBALT-SUPPORT COMPOUND IN Co/TiO_2 CATALYST

It has been known that the Co/TiO_2 catalyst is considered to have strong metal support interaction (SMSI) and shows high activities in CO hydrogenation [92,93]. This interaction is an important factor used for determining the properties of Co/TiO_2 catalyst such as cobalt dispersion and reduction behavior [97]. In fact, the synthesis of highly dispersed cobalt on TiO_2 support requires the strong interaction between cobalt and support. However, too strong interaction can produce the Co-support compound as a suboxide at an interface that is high resistant to reduction [98,99]. Jongsomjit et al. [101] reported Co-support compound formation (Co-SCF) during standard reduction resulting in a lower reducibility of Co/TiO_2 catalyst. The compound of cobalt and TiO_2 formed referred as "Co-titanate" was considered to be non-reducible form and it revealed that this "Co-titanate" formed was likely to be different from $CoTiO_3$. It was also reported that Co-SCF in SiO_2 and Al_2O_3 can occur during standard reduction and resulted in a lower reducibility of catalyst [107]. In case of TiO_2-supported cobalt, although, it has been known that the dominant surface sites of TiO_2 support consist of two main sites as Ti^{4+} and Ti^{3+} [14,15,17,18], the effect of surface sites on the formation of Co-SCF has not yet been investigated as well. In our previous chapter, the impact of Ti^{3+} present in TiO_2 support on catalytic properties of Co/TiO_2 has been discussed. Therefore, in this work, the proposed research, we aim to extend the investigation to the cobalt-support compound formation on such catalyst. The effect of surface sites (as a Ti^{4+} and Ti^{3+} on TiO_2 support) on the cobalt-support compound formation has been investigated as the main goal. Furthermore, the simple chemical form and the mechanism to form the Co-SCF have also been proposed by means of electron spin resonance spectroscopy (ESR). The nomenclatures used for the Co/TiO_2 catalysts in this study are following:

- A, B, C, D : The supported cobalt on TiO_2 which had a Ti^{4+}/Ti^{3+} molar ratio covering on the surface of 1.2, 1.3, 1.4, and 1.6, respectively.

9.1 Effect of surface sites (Ti^{4+} and Ti^{3+}) of TiO_2 support on the formation of Co-SCF in Co/TiO_2 catalyst.

TiO_2 support having a difference of Ti^{4+} to Ti^{3+} covering ratios on the surface has been prepared following our previous chapter. Based on CO_2-TPD technique monitoring surface sites of TiO_2 (Original by Thomson et al. [39]), the Ti^{4+}/Ti^{3+} ratios were estimated from the ratio between the CO_2 desorption peak at temperature 175 K (Ti^{4+} site) and 200 K (Ti^{3+} site). The four TiO_2 supports with a difference of Ti^{4+}/Ti^{3+} ratios on the surface (1.2, 1.3, 1.4, and 1.6) were prepared as indicated in the Table 9.1. The infrared spectroscopy (IR) (Figure 9.1(A)) characterizing the OH group bonding to Ti^{4+} site and Ti^{3+} site of the three TiO_2 supports of the sample A, B, and D was also used to confirm the Ti^{4+}/Ti^{3+} ratios. As seen in the Figure 9.1(B), all IR spectra exhibited mainly two OH peaks at υ_{OH} = 3717 and 3673 cm^{-1}. Based on the report of Szczepankiewicz et al. [108], the IR peak at υ_{OH} = 3717 cm^{-1} represented the OH bonded to Ti^{3+} site on the surface of TiO_2 support. In case of the IR peak at υ_{OH} = 3673 cm^{-1}, it was assigned to be the OH bonded to Ti^{4+} site [109,110]. Compared among the IR spectra of TiO_2 supports used for preparing Co/TiO_2 in the sample A, B, and D [as seen in the Figure 9.1(B)], showing that the intensity of the band characterizing Ti^{3+}-bonded OH species (υ_{OH} = 3717 cm^{-1}) decreased relatively with the number of Ti^{4+}-bonded OH groups (υ_{OH} = 3673 cm^{-1}). The Ti^{4+}/Ti^{3+} ratios covering on the surface TiO_2 support, estimated from the ratio between the IR peak at υ_{OH} = 3671 and υ_{OH} = 3717 cm^{-1}, were also summarized in the Table 9.1. It shows that the trend of the Ti^{4+}/Ti^{3+} ratios covering on TiO_2 support has a good agreement with those from CO_2-TPD results.

Table 9.1: Characteristics of TiO_2 supports and Co/TiO_2 catalysts

Sample	TiO_2 support			Co/TiO_2 catalyst				
	Ti^{4+}/Ti^{3+} ratio[a]	Ti^{4+}-OH/Ti^{3+}-OH ratio (IR)[b]	Ti^{3+} (ESR)[c]	% Reducibility[d]	TPR Temp. (K)[e]	H_2-chemisorb (10^7 molecule/g)	% Co dispersion[f]	Reaction rate[g] (mmol g^{-1} s^{-1})
A	1.2	0.8	3631	66	738	16.8	1.7	18
B	1.3	1.2	3024	51	729	16.2	1.6	15
C	1.4		2898	48	800	11.4	1.1	13
D	1.6	1.4	2885	35	859	9.6	0.9	11

[a] Calculated from CO_2-TPD spectra.

[b] The ratio between the intensity of IR spectra at υ_{OH} = 3670 cm^{-1} (Ti^{4+}-OH) and υ_{OH} = 3716 cm^{-1}(Ti^{3+}-OH).

[c] The intensity of ESR spectra at g value 1.996.

[d] Calculated from Temperature-Programmed-Reduction (TPR).

[e] The temperature at the maximum peak of TPR.

[f] Calculated from H_2-chemisorption.

[g] Rate of CO hydrogenation after 4 h.

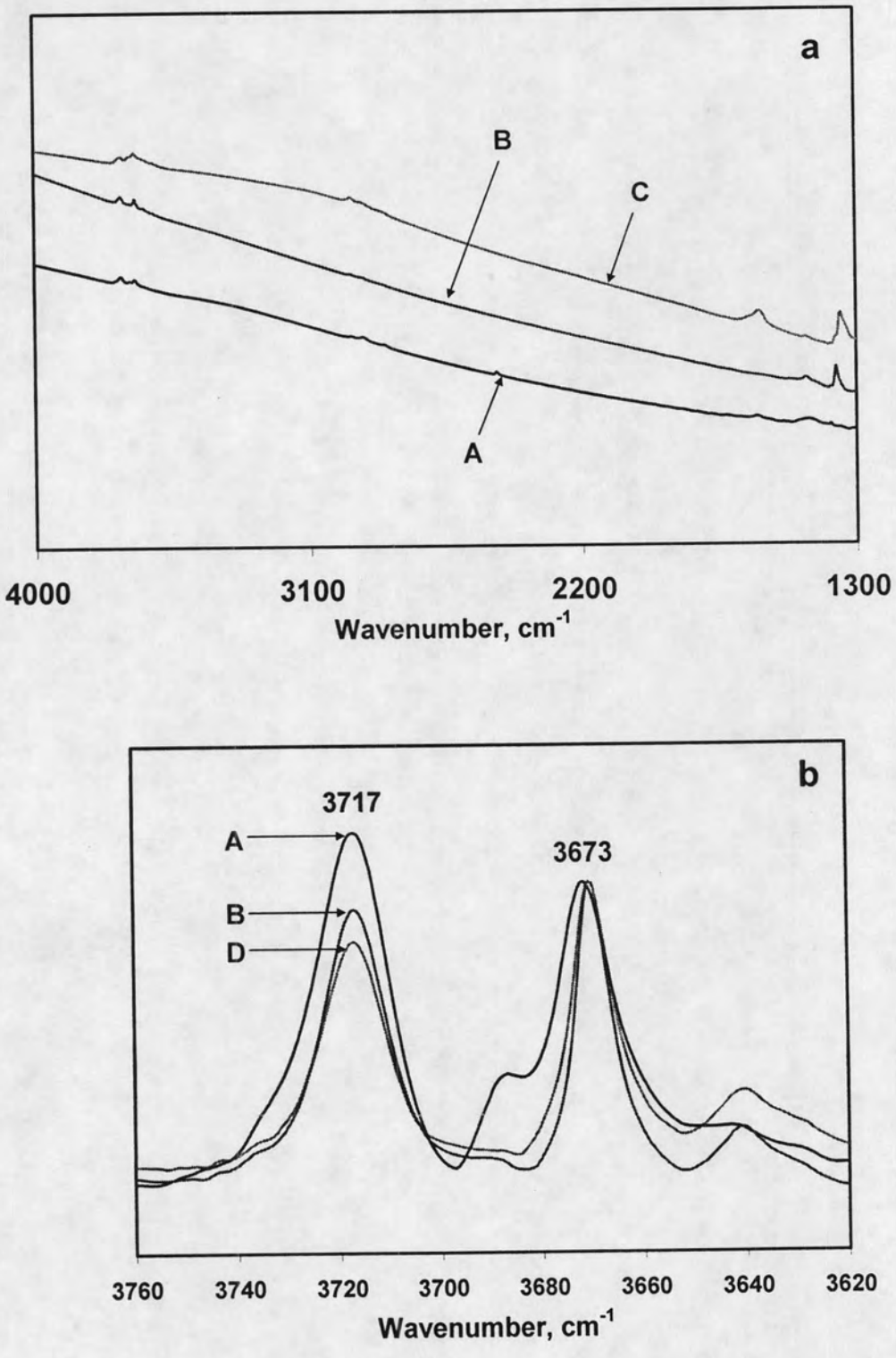

Figure 9.1: The infrared spectroscopy: (a) characterizing the TiO2 supports (prior to cobalt loading) used for sample A, B, and C; (b) considering on the OH region

The electron spin resonance spectroscopy (ESR) as seen in the Figure 9.2(A) was also used for confirming the quantitative data from CO_2-TPD and IR, the ESR spectra, performing at 77 K without illumination on samples, exhibited mainly one signal at the g value of 1.996 for all samples meaning Ti^{3+} site. Based on intensity of ESR spectra as summarized in the Table 9.1 (which is corresponding to the amounts of Ti^{3+} present in TiO_2 surface), it shows that a decrease of the amount of Ti^{3+} corresponded well with an increasing of the Ti^{4+}/Ti^{3+} ratios obtained from CO_2-TPD and IR .

A 20 % cobalt has been prepared on each TiO_2 supports which had a difference of Ti^{4+}/Ti^{3+} ratios covering on the surface (1.2, 1.3, 1.4, and 1.6 based on CO_2-TPD). The characteristics of each Co/TiO_2 catalyst have been summarized in the Table 9.1. Considered on the % reducibility, when the most proportion of surface site on TiO_2 support became Ti^{4+} site (from A to B, C, and D, consequently), the Co/TiO_2 catalyst changed to be a harder reductive catalyst (Co^{3+} reduced to Co^{2+}, and then reduced to Co^0 in final step) as seen by the decreasing of % reducibility. This is because more amount of non-reducible compound as a Co-SCF was formed on the Co/TiO_2 catalyst [101,107]. The reducibility loss (based on sample A) during the standard reduction process was found to be in the range of 8 (for sample B) to 47 % (for sample D). Based on the TPR profiles as shown in the Figure 8.6, it indicates that the reduction peaks (overlap of Co^{3+}> Co^{2+} > Co^0) shifted to higher temperature when the most proportion on the surface of TiO_2 support became Ti^{4+} site (the changing of temperature was summarized in the Table 1) confirming the existence of Co-SCF on Co/TiO_2. Combined between the % reducibility loss and the moving to higher temperature of TPR profiles, it can be concluded that the non-reducible compound as a Co-SCF preferred to form on the surface of Co/TiO_2 catalyst, when the TiO_2 support had more Ti^{4+} covering on the surface. Based on the two dominant surface sites of TiO_2 support as a Ti^{4+} and Ti^{3+} sites [14,15,17,18], on the other hand, it can be referred that the Co-SCF preferred to form at the Ti^{4+} site, but more characterization is still needed to confirm this proposal.

There are many reports showing the effect of surface site as a Ti^{4+} and Ti^{3+} on the adsorption of metal and oxide, as summarized by Diebold [14]. It has been known that the bond energy for anchoring of the metal is stronger at the Ti^{3+} site than at the Ti^{4+} [104]. This is because the Ti^{3+} has one lone pair electron at ***d*** orbital resulting in the higher reactive with the metal and oxide loading [14]. Based on this bond energy, Wallace et al. summarized the role of Ti^{3+} site on Au cluster nucleation, growth, and stability on Ti^{3+} site of TiO_2 support [33]. It showed that an increase of Ti^{3+} site strongly decreases the rate of Au cluster migration during high temperature condition due to the strongly bonding between Ti^{3+} site and Au cluster. The reports showing the strong bonding between Gr. VIII metals and Ti^{3+} have been done by many researchers [14,111,112]. In this work, based on this bond energy, Ti^{3+} on the surface of TiO_2 support should have the responsibility for fixing the cobalt cluster on the support resulting in a decrease of cobalt migration for forming a bigger cobalt size. This suggestion can be confirmed by the changing of the cobalt dispersion on the surface of TiO_2 support as indicated in the Table 9.1. It reveals that the increase of cobalt dispersion can be observed when the surface of TiO_2 support has more Ti^{3+} sites. This increase of cobalt dispersion due to the Ti^{3+} site can inhibit the agglomeration between cobalt clusters by the decreasing the migration rate of clusters. Zhang et al. [99] mentioned the effect of cobalt migration on the formation of Co-SCF, they investigated the reducibility of Co-Ru/γ-Al_2O_3 during standard reduction in the presence of added water vapor. They reported that the migration of cobalt played the significant role for the forming of Co-SCF. In this work, the results showing the existence of Co-SCF with the observing the decrease of cobalt dispersion corresponded well with the conclusion of Zhang et al. [99]. Therefore, it can be suggested that the non-reducible compound, as the Co-SCF preferred to form on Co/TiO_2 catalyst having more Ti^{4+} site on the support due to the increasing of cobalt migration rate.

9.2 Determination of Co-SCF characteristics

Based on the previous work in our laboratory, Jongsomjit et al. also investigated to identify the nature of Co-SCF on Co/TiO_2 catalyst using several characterization techniques including SEM-EDX, XRD, and Raman spectroscopy [101]. In cased of SEM-EDX and XRD, it can not detect a Co-SCF on the Co/TiO_2 because this compound has highly dispersed form. However, Raman spectroscopy revealed that this highly dispersed Co-SCF formed was likely to be different from $CoTiO_3$ and present as the more complex derivatives on Co/TiO_2 catalyst. It should be noted that, however, the Co-SCF has still never been directly detected by any techniques. In order to determine the nature of cobalt compound as more complex derivatives from the interaction between cobalt and the other metal compound, the electron spin resonance has been used by many researchers [113-117]. Schmidt et al. [117] investigated the nature of cobalt complexes in Ziegler type catalytic system using ESR and reported that the reduction of cationic cobalt to the zero-valent state can facilitate the formation of paramagnetic Co(II) and Co(0) complexes. However, in case of Co/TiO_2 catalyst used for hydrogenation reaction, the evidence of Co-SCF by monitoring of ESR has never been done so far. Therefore, in this work, we tried to use the ESR spectroscopy, as a promising technique, for probing the evidence of Co-SCF on Co/TiO_2 catalyst. In this work, the ESR investigation Co/TiO_2 catalyst prior standard reduction, and Co/TiO_2 catalyst after standard reduction were performed to investigate the Co-SCF complexes.

The ESR spectra of supported cobalt on TiO_2 with the different Ti^{4+}/Ti^{3+} ratios (A, B, and D samples) prior to standard reduction was shown in the Figure 9.2(B). Based on analysis over all range of magnetic field (unit in Mt), it can detect only the small peak at g value ca. 1.995 which can assign to be Ti^{3+} site on TiO_2 support. Based on the disappearance of Ti^{3+} site on the surface of TiO_2 support [between Figure 9.2(A) and (B)] , it shows that almost Ti^{3+} sites were used and participated to anchor the cobalt cluster on TiO_2 support resulting in an increase of cobalt dispersion as discussed in the previous section. However, it should be further mentioned that, based on result from % reducibility loss with increased Ti^{4+} sites, some of cobalt cluster should be participated to anchor at

Ti^{4+} site as well. From the spectra, it can not detect any paramagnetic cobalt species as a Co(II) and Co(0) on these catalyst at g value ca. 2.16 and 1.41, respectively [115]. Based on this analysis of Co/TiO_2 prior to standard reduction, although, the Co/TiO_2 was dried at 383 K for 12 h and calcined in air at 723 K for 4 h during catalyst preparation, it shows that any cobalt compound as more complex derivatives from the interaction between cobalt and TiO_2 support was not present. This shows that something is missing for the formation of the Co-SCF.

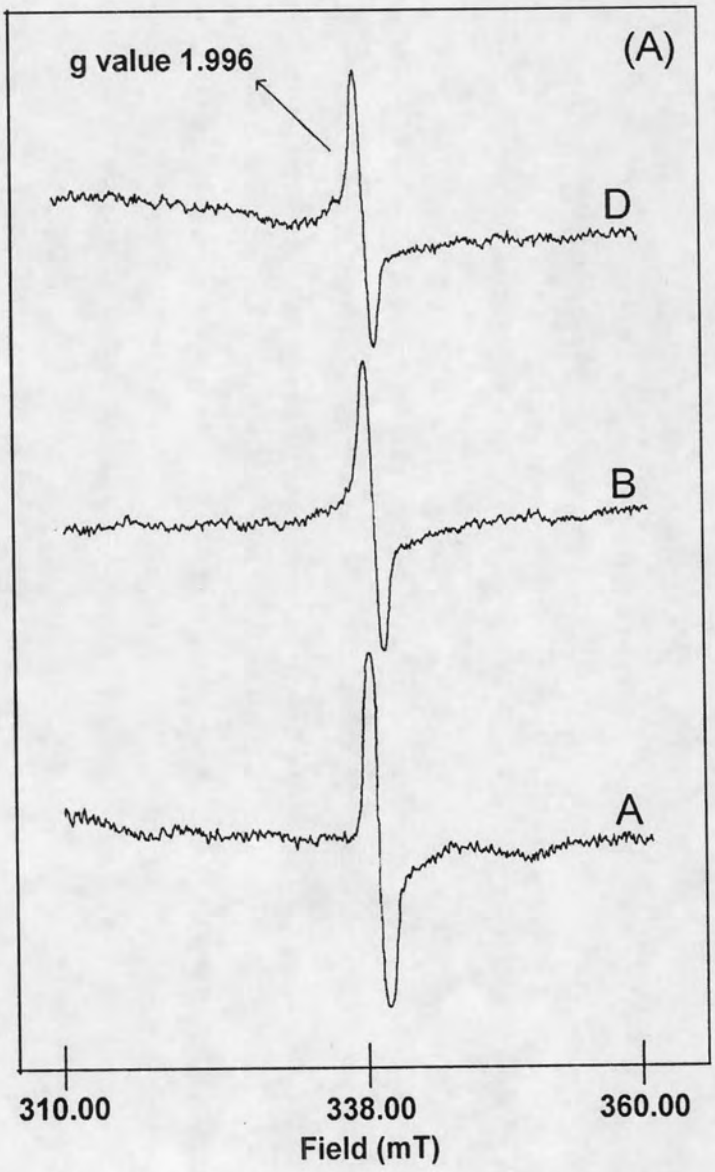

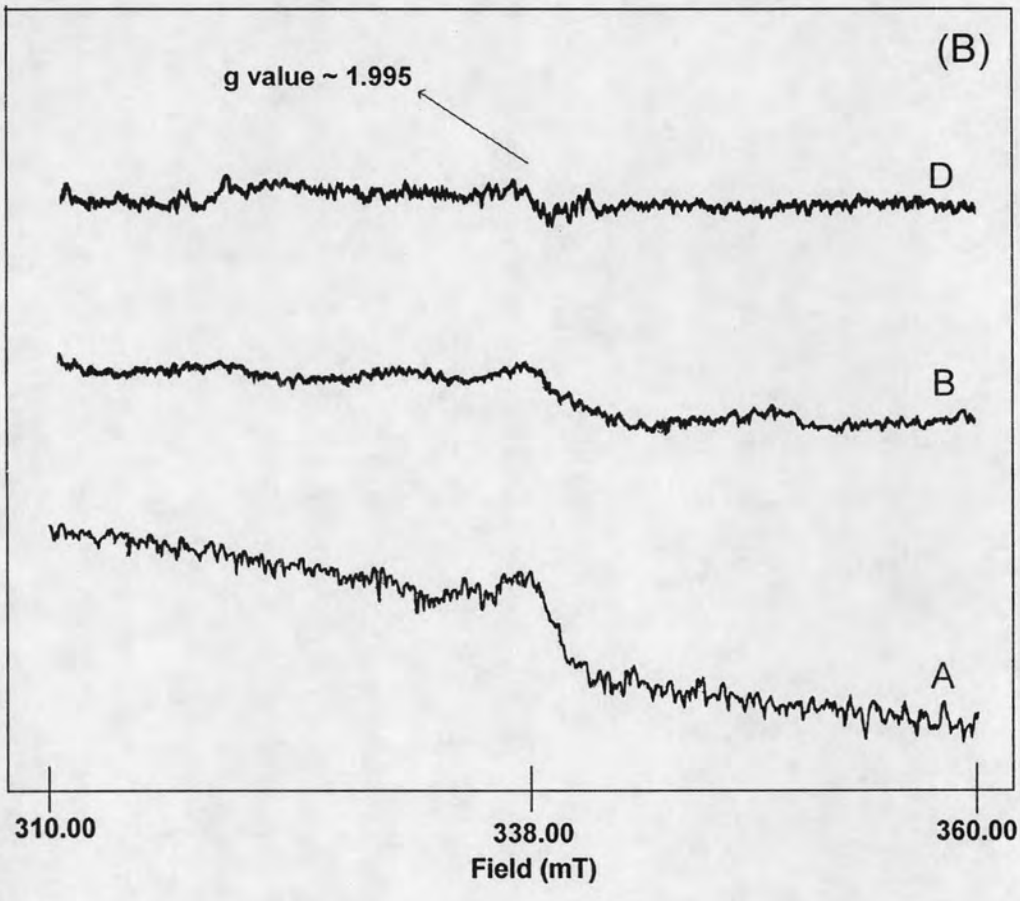

Figure 9.2: ESR spectra (A) before and (B) after cobalt loading on TiO_2 supports

The ESR analysis of supported cobalt on TiO_2 support with the different Ti^{4+}/Ti^{3+} ratios (A, B, and D samples) after standard reduction was also performed as shown in the Figure 9.3(C), 9.4(A), and 9.4(B). It can be observed that these spectra were very different from the spectra of Co/TiO_2 prior standard reduction. These spectra could be assigned as a Co-SCF on the Co/TiO_2 catalyst. Therefore, this was suggested that the formation of Co-SCF can be facilitated by the presence of hydrogen during reduction. Based on ESR theory, this spectra were the hyperfine patterns which results in multi-peak ESR spectra [118,119].

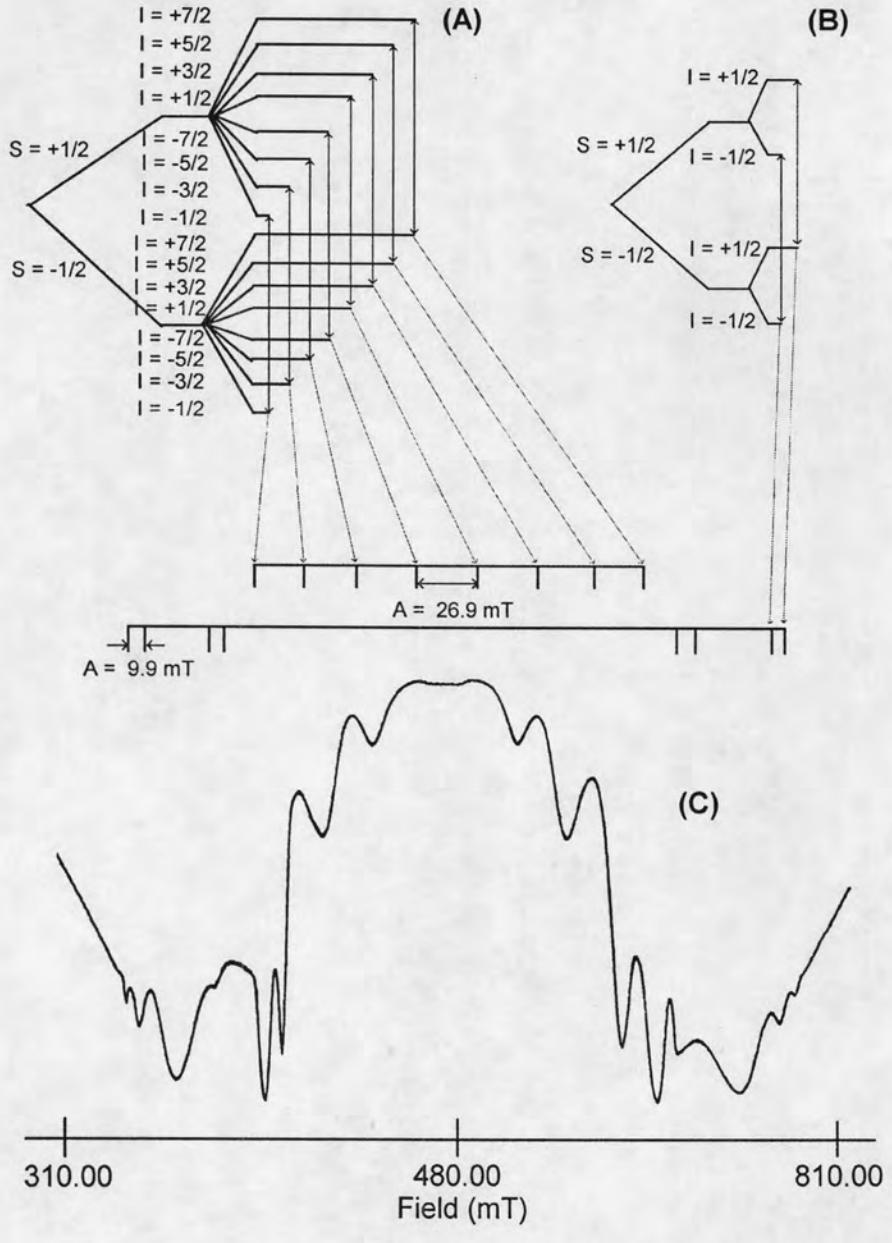

Figure 9.3: The consistency between the theory and experimental result to form the hyperfine pattern of Co-SCF after standard reduction. (A) The theory showing the contacting between one lone pair electron ($S = \pm 1/2$) and the nucleus of ^{59}Co ($I = \pm 7/2$). (B) The theory showing the contacting between one lone pair electron ($S = \pm 1/2$) and the nucleus of ^{1}H ($I = \pm 1/2$). (C) The experimental results from ESR spectrum of sample A after standard reduction obtained at 77 K in vacuum without irradiation

This hyperfine pattern can occur when a lone pair electron (half electron spin) contacts with at lease one nucleus (one nuclear spin) [114,120,121]. The cobalt can be classified to be a low-spin Co(II) with a d^7 electron configuration or Co(0) with a d^9 electron configuration [114]. Based on this electron configuration, the one lone pair electron in ***d*** orbital of both cobalt can be considered to be S = ±1/2 (haft spin of lone pair electron) [120]. Also nuclear spin, cobalt have I = ±7/2 indicating ^{59}Co with abundance of 100 % in the nature [122]. Based on Figure 9.3(A), when one lone pair electron (S = ±1/2) in the ***d*** orbital contacts with one nucleus of ^{59}Co with I = ±7/2, eight peaks of hyperfine pattern, which symmetrically spitted from center of one lone pair electron in ***d*** orbital of cobalt (S = ±1/2), will occur [114,120,121]. Considered on the hyperfine pattern of sample A as also seen in the Figure 9.3(C), the well consistency between the experimental showing hyperfine pattern and ESR theory can be observed in this sample. It was showed that there are eight peaks symmetrically spitted, with equal distance of ***A*** = 26.9 Mt, from the central peak at ***g*** = 1.049 (as summarized in the Table 3). This center attributed to the electron spin of one lone pair electron (S = ±1/2) in ***d*** orbital of Co(0) [115]. Based on the consistency between the hyperfine pattern from experimental and theory, it can be mentioned that non-reducible compound formed after standard reduction had a form of Co(0) compound. In this hyperfine pattern, there are two patterns in hyperfine spectra (as seen in the Figure 9.3(C)), one is attributed to^{59}Co with a larger ***A*** value and the smaller one (***A*** = 9.9 Mt) of four sets of two sub-hyperfine patterns. Saraev et al. [114] also found the two patterns in hyperfine spectra of $Co(acac)_2$-Pbu_3-complexes. One was the eight lines of a ^{59}Co (I = ±7/2) with a larger ***A*** value and the smaller one of ***A*** value (of two sub-hyperfine peak) which was attributed to ^{31}P (I = ±1/2). The two sub-hyperfine patterns came from the contacting of one lone pair electron (S= ±1/2) with one nucleus of I = ±1/2 as seen in the Figure 9.3(B) [114]. Based on the system of this Co/TiO_2 catalyst after standard reduction with hydrogen, these two sub-hyperfine patterns should come from the nucleus of ^{1}H (I = ±1/2) with abundance of 99.98 % in nature [123]. It can not come from the nucleus of ^{47}Ti and ^{49}Ti (abundance of 7.44 and 5.41 %, consequently) because they really have the less abundance in the nature. And if it came from ^{47}Ti and ^{49}Ti, these sub-hyperfine pattern must have six or eight lines (with equal of distance from center) of I = ±5/2 and ±7/2, respectively [124]. These four

sets of ^1H can be classified to be a two symmetrical pattern with a distance from central peak equal to A = 112.5 and 154.2 Mt (as summarized in the Table 3) showing a uniform structure of Co-SCF. As mentioned above, however, the occurring of two sub-hyperfine patterns must have one lone pair electron from some source contacting with one nucleus of ^1H [114,123]. Considered in this system of Co/TiO_2 catalyst, this lone pair electron can come from ***d*** orbital of TiO_2 support [14]. Therefore, based on the hyperfine pattern of ESR spectra, we suggested that the non-reducible compound as a Co-SCF should have the simple chemical form (which consisted of one Co(0), four ^1H, and one TiO_2) as a $Co^0(H_4TiO_4)$.

The ESR spectra of sample B and D were also presented in the Figure 9.4(A) and 9.4(B), respectively. The hyperfine pattern of sample B and D still had the same pattern with that of sample A. Eight lines of Co(0) can still be observed with the four set of two sub-hyperfine patterns from ^1H. When surface of TiO_2 had more Ti^{4+}, the Co-SCF occurred still had the same basic chemical form as a $Co^0(H_4TiO_4)$. However, when the surface of TiO_2 had more Ti^{4+} site, the loss of symmetrical pattern can be observed indicating the occurring of non-uniform structure (considered on the Figure 9.4(A) and 9.4(B) and also the error of hyperfine pattern as summarized in the Table 9.3). In case of sample B and D, the center of peak still around 1.409, however, the average spitting distance of eight line of Co(0) became more asymmetry (considered at the error) when the TiO_2 had more Ti^{4+} sites. Considered on the distance from center of two sub-hyperfine patterns, it should be mentioned that the changing of these distance of ^1H to be more asymmetry attributed to the occurring of the random bonding position of hydrogen atom in Co-SCF structure [125]. The observation of non-symmetric set of two sub-hyperfine patterns in the sample D, at A = 107.3 Mt (left), 87.5 Mt (left), 62.5 Mt (left), 108.3 Mt (right), and 77 Mt (right), can also use to confirm the random bonding position of hydrogen atom resulting in the non-uniform structure of Co-SCF. Therefore, this proposed chemical form as a $Co^0(H_4TiO_4)$ is only a elementary proposed form because more asymmetry and the random peaks can be observed when the surface of TiO_2 support having more Ti^{4+}. Therefore, in this work, Co-SCF should be represented on the basic chemical form a $Co^0(H_xTiO_y)$, where x corresponded to the number of two sub-hyperfine

patterns and y is the number of oxygen that present for balancing the total oxidation number of this compound to be a zero.

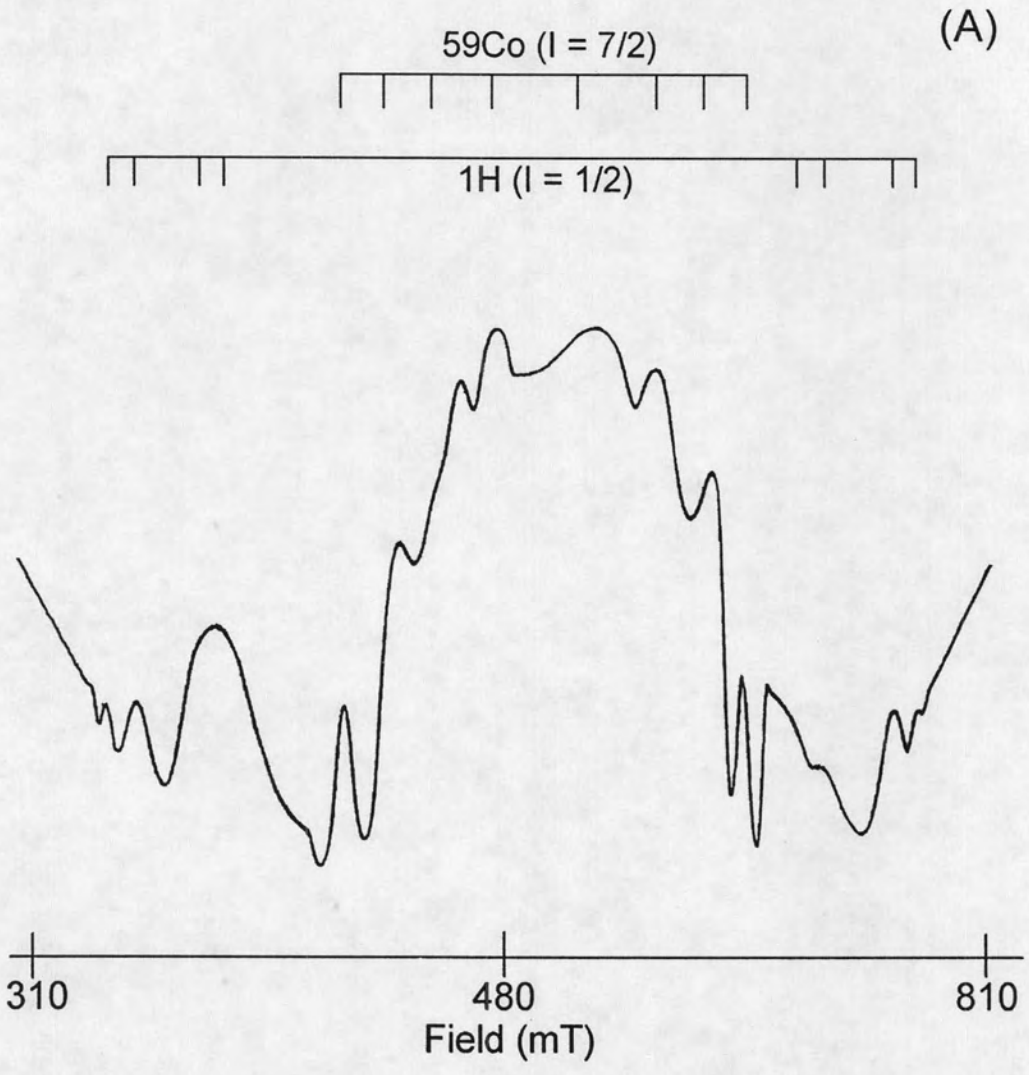

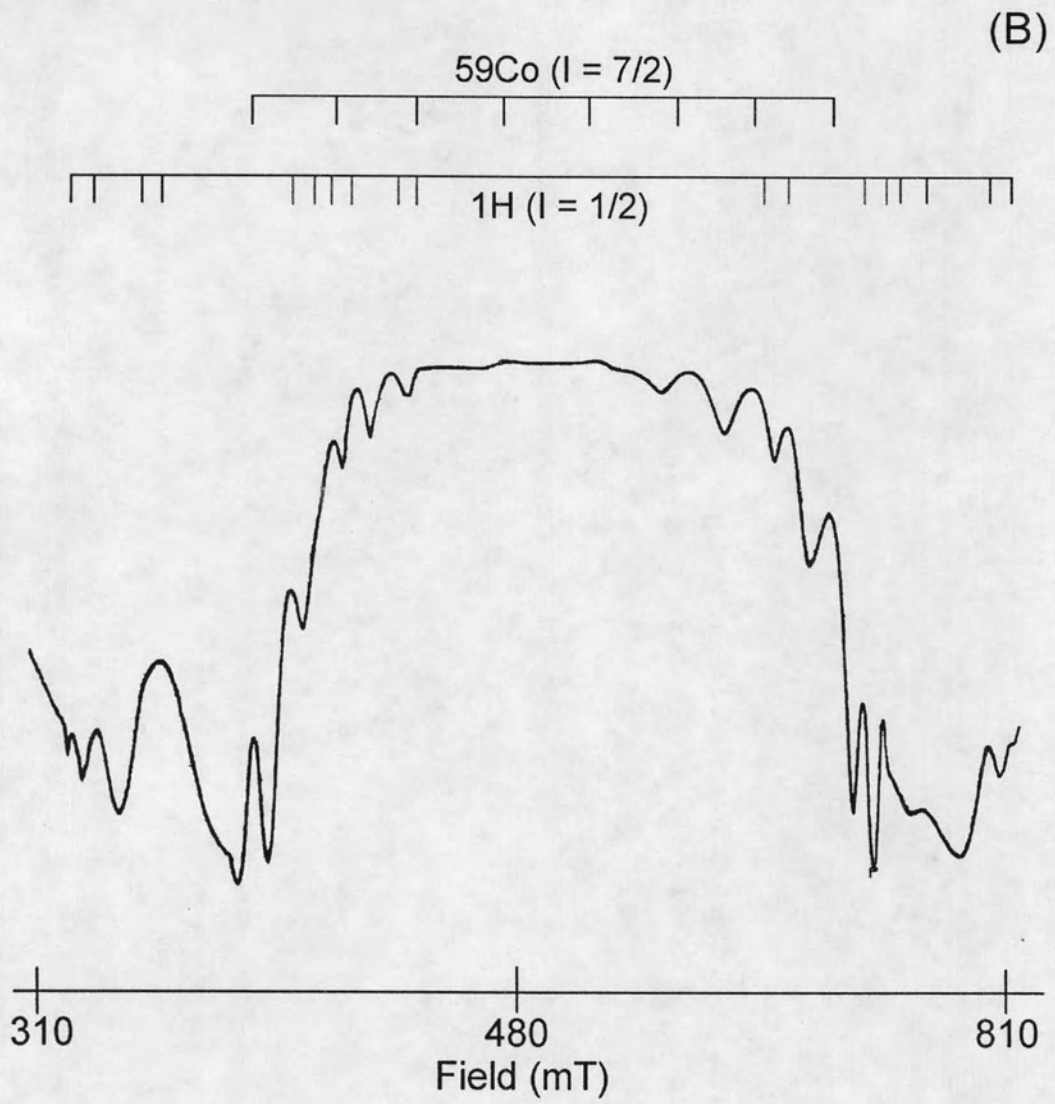

Figure 9.4: ESR spectra of Co/TiO_2 after standard reduction obtained at 77 K in vacuum without irradiation of samples (A) B and (B) D

Table 9.3: Parameters of the hyperfine pattern from ESR spectra of Co/TiO_2 after standard reduction.

		Cobalt (I=7/2)[a]	^1H (I=1/2)	
Sample	Centric g tensor	A tensor (Mt)	A tensor (Mt)[b]	Distance from center (Mt)[c]
A	1.409	26.9 ± 0.09	9.9 ± 0.05	(i) 112.5 ± 0.00, (ii) 154.2 ± 0.05
B	1.392	21.1 ± 0.11	10.7 ± 0.12	(i) 105.2 ± 0.11, (ii) 130.5 ± 0.08
D	1.401	30.0 ± 0.16	9.1 ± 0.03	(i) 126.0 ± 0.07, (ii) 160.7 ± 0.01

[a] Calculated from the average 8 peaks of ^{59}Co (I=7/2)

[b] Calculated from the average 4 set of two sub-hyperfine patterns of ^1H (I=1/2)

[c] Indicating mainly two symmetrical patterns of ^1H (I=1/2)

Briefly, many researchers mentioned that CoM_xO_{3+x} (where x = 1, 2,... and M = metal element of support such as Ti, Si) should be the main form of Co-SCF (the details have been summarized in the Table 9.2) [99,101,126,127,128,129,130]. Jongsomjit et al. [101] also mentioned about this chemical form of Co-SCF, they reported that the form of Co-SCF seems different from the CoM_xO_{3+x} compound. Therefore, it seems that Co-SCF might have many possible chemical structures. However, in this work, based on the promising ESR technique, the simple chemical form of Co-SCF as a $Co^0(H_xTiO_y)$ should be one choice of a possible model for studying the formation of Co-SCF. However, there are the important question that "How can this compound occur?". We tried to find out this question using proposed pathway mechanism as seen in the simplified Scheme 9.1. There are two possibly simplified pathways to form this compound during standard reduction. In the pathway A, it have two sub-path way are as follows: (i) the cationic cobalt (Co(III) and Co(II)) are reduced with hydrogen to form zero-valent cobalt and then (ii) this zero-valent cobalt is facilitated by hydrogen to interact with the TiO_2 support and form the Co(0) compound. In addition, based on the pathway B, the cationic cobalt migrate on Ti^{4+} site of the surface of TiO_2 support and agglomerate to form metallic cobalt (zero-valent cobalt) coinciding with the interaction with TiO_2 support using hydrogen facilitation and form the Co(0) compound as a non-reducible Co-SCF. However, based on the previous section, the pathway A contradicts with the result of the % reducibility since if it accords with this pathway, it must consume the equal amount of hydrogen, but somehow it does not. Therefore, the possible pathway should be the pathway B which competes with the activation of cobalt (to form the active cobalt) by hydrogen reduction (as seen in the Activation Pathway in Scheme I). It should be mentioned that the competition between activation pathway and deactivation pathway resulted in a decrease of % activity (as seen in the Table 9.1.) when the Ti^{4+} covering on the surface of TiO_2 support increased.

Table 9.2: The supposed structure of cobalt-support compound formation by many research works.

Sample	Cobalt-support compound formation		Ref.
	The supposed structure after standard reduction	The detection on the sample after standard reduction	
Co/Al_2O_3	Cobalt aluminate as a $CoAl_2O_4$	c.d.*	31, 35
$Co\text{-}Ru/Al_2O_3$	Cobalt aluminate as a $CoAl_2O_4$	c.d.	5, 32
$Co/Zr\text{-}Al_2O_3$	Cobalt aluminate as a $CoAl_2O_4$	c.d.	33
Co/SiO_2	Cobalt silicate as a $CoSiO_3$	c.d.	34
Co/TiO_2	Cobalt titanate as a $CoTiO_3$	c.d.	6, 35
Co/TiO_2	$Co^0(H_xTiO_y)$	Electron spin resonance spectroscopy (ESR)	This work

*c.d. = can not detect

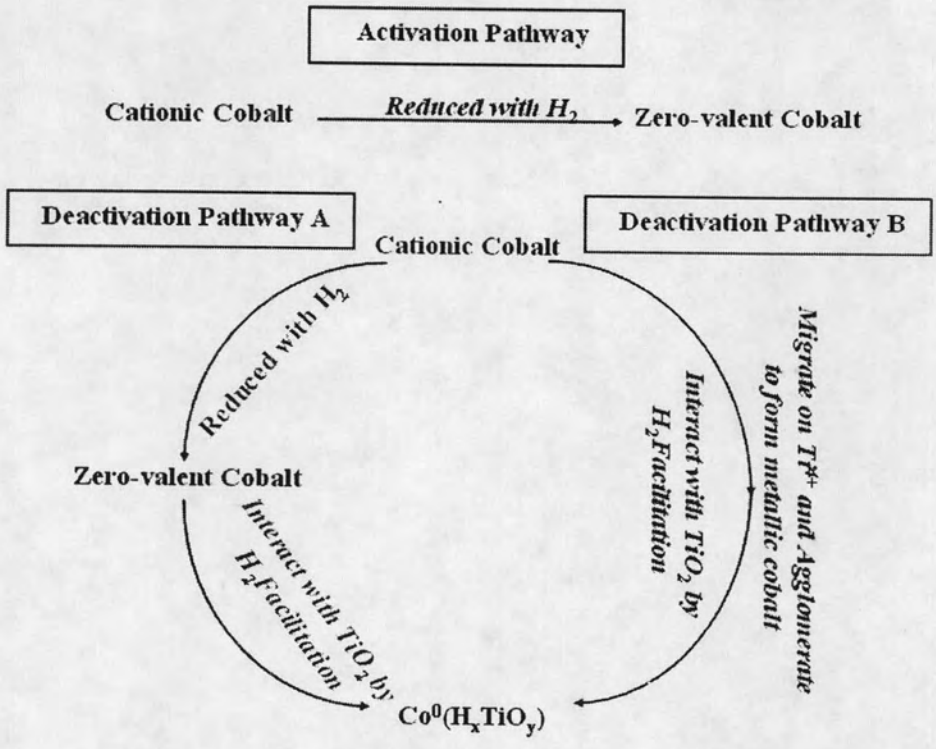

Scheme 9.1: The simplified mechanism of the $Co^0(H_xTiO_y)$ compound formation